Development of fast neutron pinhole camera using nuclear emulsion for neutron emission profile measurement in KSTAR

Y. Izumi, H. Tomita, Y. Nakayama, S. Hayashi, K. Morishima, M. Isobe, M. S. Cheon, K. Ogawa, T. Nishitani, T. Naka, T. Nakano, M. Nakamura, and T. Iguchi

Citation: Review of Scientific Instruments **87**, 11D840 (2016); doi: 10.1063/1.4963866
View online: http://dx.doi.org/10.1063/1.4963866
View Table of Contents: http://aip.scitation.org/toc/rsi/87/11
Published by the American Institute of Physics

REVIEW OF SCIENTIFIC INSTRUMENTS **87**, 11D840 (2016)

Development of fast neutron pinhole camera using nuclear emulsion for neutron emission profile measurement in KSTAR

Y. Izumi,[1] H. Tomita,[1,a)] Y. Nakayama,[1] S. Hayashi,[1] K. Morishima,[1] M. Isobe,[2,3] M. S. Cheon,[4] K. Ogawa,[2,3] T. Nishitani,[2] T. Naka,[1] T. Nakano,[1] M. Nakamura,[1] and T. Iguchi[1]

[1]*Nagoya University, Furo-cho, Chikusa-ku, Nagoya 464-8603, Japan*
[2]*National Insuitute for Fusion Science, 322-6 Oroshi-cho, Toki 509-5292, Japan*
[3]*SOKENDAI (The Graduate University for Advanced Studies), 322-6, Oroshi-cho, Toki 509-5292, Japan*
[4]*Diagnostics Technology Team, ITER Korea, National Fusion Reseach Institute, Daegeon 305-333, South Korea*

(Presented 7 June 2016; received 3 June 2016; accepted 15 September 2016; published online 4 October 2016)

We have developed a compact fast neutron camera based on a stack of nuclear emulsion plates and a pinhole collimator. The camera was installed at J-port of Korea superconducting tokamak advanced research at National Fusion Research Institute, Republic of Korea. Fast neutron images agreed better with calculated ones based on Monte Carlo neutron simulation using the uniform distribution of Deuterium-Deuterium (DD) neutron source in a torus of 40 cm radius. *Published by AIP Publishing.* [http://dx.doi.org/10.1063/1.4963866]

I. INTRODUCTION

Fast MeV neutrons (Deuterium-Deuterium (DD) neutrons) are generated by DD fusion reaction in magnetically confined deuterium plasma with neutral deuterium injection heating at experimental fusion devices. During neutral beam injection heating, the reaction between fast deuterium ions and thermal deuterium ions is dominated in the deuterium plasma because of the energy dependence of its cross section. Thus, nuclear fusion neutron measurement provides significant information of fast ion behavior and its confinement in high-temperature plasma. DD neutron emission profile measurement is important to understand fusion source, i.e., its location, shape, and intensity. The conventional emission profile monitor is based on line integrated measurements of the plasma (neutron source) along many lines-of-sight by array of collimators with scintillators. Although conventional massive and huge monitors have been installed on JET,[1] TFTR,[2] JT-60U,[3] etc., and are planned to be installed on ITER,[4] LHD,[5] and HL-2A,[6] a compact monitor is still demanded for relatively small experimental devices and minimum interference to other diagnostics. Previously, fast neutron detention by a nuclear emulsion, a solid-state detector sensitive to charged particle such as protons, was applied for DD neutron emission profile measurements at the Princeton large torus in 1978[7] and at ASDEX in 1990s.[8] However, a huge cost was required to analyze recorded tracks in the emulsion in these times. Then automated nuclear emulsion scanning systems were developed and it allows the wide application of the nuclear emulsion technique to fusion neutron measurement.[9–11] We have developed a compact fast neutron camera based on a stack of nuclear emulsion plates and a pinhole collimator.[12–15] The fast neutron pinhole camera using nuclear emulsion was installed at a fusion experimental device, Korea Superconducting Tokamak Advanced Research (KSTAR), at National Fusion Research Institute, Republic of Korea. In this paper, first experimental results and Monte Carlo simulation model to evaluate neutron emission profile in KSTAR are described.

II. PRINCIPLE OF FAST NEUTRON PINHOLE CAMERA

The fast neutron camera using nuclear emulsion is based on the pinhole imaging principle as described in our previous papers.[12–15] The fast neutron camera consists of nuclear emulsion plates (OPERA film,[16] 50 mm × 50 mm, 45 μm emulsion layer containing AgBr micro-crystals coated on both sides of a substrate) and a pinhole collimator made of a tungsten alloy (50 mm × 50 mm × 100 mm, acceptance angle of 10°). Fast neutrons pass through the center of pinhole collimator and then reach to nuclear emulsion plates behind the collimator. In the emulsion, a recoiled proton is generated by elastic scattering of an incident neutron with a hydrogen atom. After measurement, recoiled proton tracks are visualized in photographic development process of the nuclear emulsion. Tracks recorded in the emulsion are recognized by automated scanning system called S-UTS.[17] Neutron-gamma discrimination is possible by differences in length of these tracks. Therefore, a track density distribution of recoiled proton corresponds to a pinhole image of incident fast neutron.

Fast neutron pinhole image is given as a convolution of an emission profile of neutron source and series of point spread function of the camera. The neutron emission profile from fusion deuterium plasma can be reconstructed by the deconvolution of the pinhole image. We have evaluated the point spread function of the camera using an accelerator based mono-energetic DD neutron point source at Fusion Neutron Source (FNS), Japan Atomic Energy Agency. The experimental responses were consistent with the simulated

Note: Contributed paper, published as part of the Proceedings of the 21st Topical Conference on High-Temperature Plasma Diagnostics, Madison, Wisconsin, USA, June 2016.
a)tomita@nagoya-u.jp

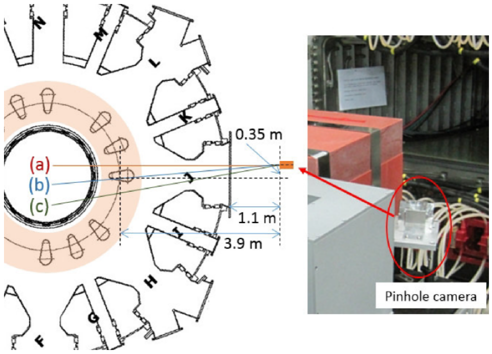

FIG. 1. Experimental setup at J-port of KSTAR. The camera set on three lines of sight, (a)–(c).

ones based on Particle and Heavy Ion Transport Code System (PHITS) in the absolute number of track density, in the shape of profile and in the peak position.

III. NEUTRON PINHOLE IMAGE IN KSTAR

We installed the pinhole camera in KSTAR for DD neutron emission profile measurement. The camera was set 3.9 m apart from center of plasma at J-port. Fig. 1 shows experimental setup including a distance from plasma and lines of sight of the camera. Several track density distributions were obtained in three lines of sight at (a) 0°, (b) −5°, and (c) −10° with respect to the normal line of J-port. The relative efficiency of pinhole camera for 2.5 MeV neutron has been estimated to be $(4.1 \pm 0.2) \times 10^{-6}$ tracks/neutron.[14] Note that each image was measured over several plasma shots with different scenarios during half day experiment typically. The track density distribution of recoiled proton recorded on nuclear emulsion (center 30 mm × 30 mm area) is shown in Fig. 2. These images (a)–(c) were obtained during shots #10447–#10487, #10488–#10717, and #10518–#10551, respectively. The number of tracks generated by fast neutrons passing through the center of pinhole collimator was 4.1×10^4, 5.8×10^4, and 6.1×10^4 tracks for images (a)–(c), respectively. 10^4 tracks are enough to obtain an image.

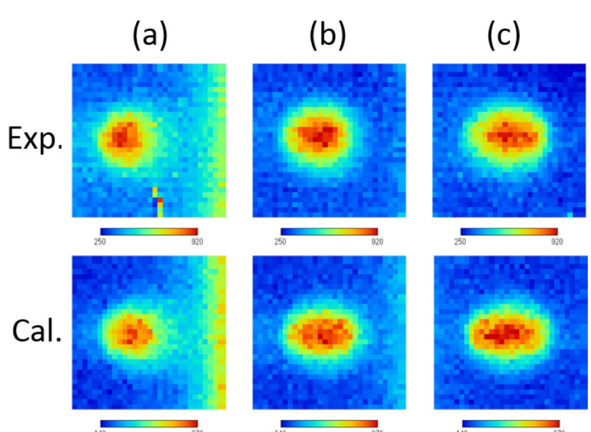

FIG. 2. Track density distributions of recoiled protons (30 mm × 30 mm). Experimental images were obtained during shots #10447–#10487 (a), #10488–#10717 (b), and #10518–#10551 (c). Calculated images using uniformly distributed DD neutron source in a torus of 40 cm minor radius are shown in bottom.

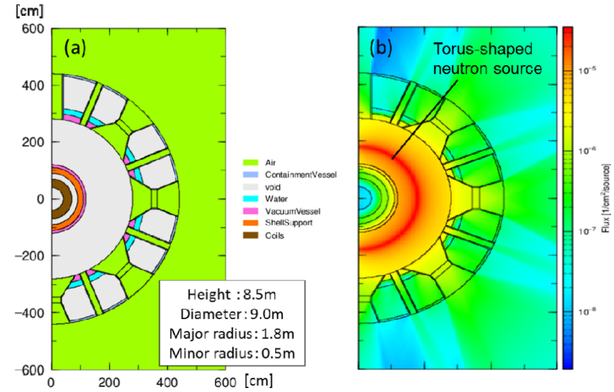

FIG. 3. Monte Carlo simulation of neutron transport in KSTAR. (a) Geometry and (b) simulation result of relative neutron flux.

To evaluate neutron emission profile in KSTAR, a Monte Carlo simulation model of KSTAR was developed based on PHITS. Fig. 3(a) shows the geometry of the model of KSTAR. Materials of vacuum vessel and superconductor coils used in the model were SUS316 and mixture of Nb_3Sn and Cu, respectively. Here, we assumed the following model of DD neutron source: mono-energetic 2.5 MeV neutrons were uniformly generated inside a torus-shaped area. Fig. 3(b) shows a typical simulation result of relative neutron flux.

Using torus-shaped neutron source which vary in minor radius r of 10, 20, 30, and 40 cm in the simulation model, the track density distributions of recoiled protons were calculated. Fig. 4 shows the comparison of the experimental image in the line of sight (c) of Fig. 1 with calculated ones with r of 10, 20, 30, and 40 cm. Fig. 5 shows line profiles of the track density distributions at the center 30 mm × 30 mm area of the emulsion, in X-direction at Y = 0 mm (left) and in Y-direction at X = 0 mm (right). The normalized mean square error (NMSE) defined below was used for quantitative comparison of the measured and calculated images,

$$\text{NMSE} = \frac{\sum \left(g\left(x, y\right) - f\left(x, y\right)\right)^2}{\sum f(x, y)^2}, \qquad (1)$$

where f is the experimental image and g is the calculated image. NMSEs between the experimental image and the simulation ones were estimated to be 0.064, 0.040, 0.026, and 0.009 for r = 10, 20, 30, and 40 cm, respectively. As a result of the NMSE evaluation, the calculated result using the uniform distribution of DD neutron source in a torus of 40 cm minor radius agrees better with the experimental results. Calculated images using uniformly distributed DD neutron source in a torus of 40 cm minor radius for three lines of sight (a)–(c) are also shown in Fig. 2. Since the tracks refer to different plasma

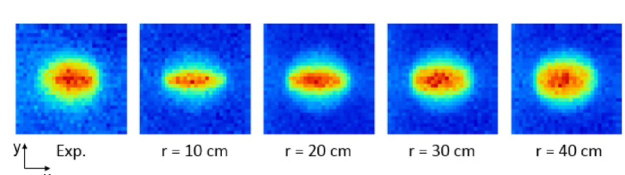

FIG. 4. Comparison of the experimental image in the line of sight (c) in Fig. 1 with calculated ones using torus-shaped neutron source with r of 10, 20, 30, and 40 cm.

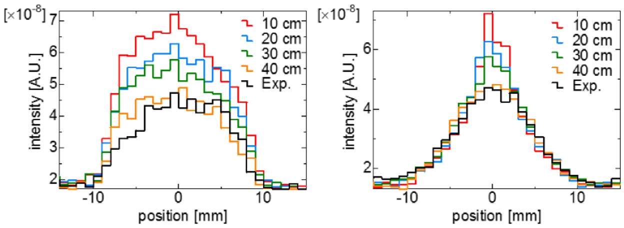

FIG. 5. Line profile of the distribution of recoiled proton tracks at the center 30 mm × 30 mm area of the emulsion in line of sight (c) in Fig. 1, X-direction at Y = 0 mm on the left and in Y-direction at X = 0 mm on the right.

scenarios, the experimental images represent average plasmas conditions during those experimental sessions. Therefore, the discrepancies in NMSEs for r = 10–40 cm are not only caused by the simplified DD neutron source model used in the calculations. In order to have better comprehension between the experimental and calculated images, this method should be used for similar shots during the session so that the DD neutron source could be better tuned and be more representative of the plasma conditions. In addition, DD neutron source model will be improved by involving DD neutron energy spectrum and distribution based on NUBEAM code to evaluate further details of DD neutron distribution in KSTAR.

IV. CONCLUSION

We have developed a fast neutron camera based on nuclear emulsion and pinhole collimator. The camera was installed in KSTAR for DD neutron emission profile measurements. The shot integrated pinhole image of DD neutron, i.e., the track density distributions of recoiled protons, was obtained in different lines of sight of the camera. We compared the experimental image with the ones calculated by a Monte Carlo simulation model of KSTAR using uniformly distributed, 2.5 MeV mono-energetic, torus-shaped neutron source. The experimental image agreed better with calculated ones using the torus-shaped source with the minor radius of 40 cm. As future work, DD neutron source model will be improved by involving DD neutron energy spectrum and distribution based on NUBEAM code to evaluate further details of DD neutron emission profile in KSTAR. In addition, image reconstruction algorithm is under development for tomographic image of neutron emission profile.

ACKNOWLEDGMENTS

This work was performed with the support and under the auspices of the NIFS Collaboration Research program (Grant Nos. NIFS12KOAH029, NIFS15KOAH033, NIFS11KLEH011, and NIFS14KLEH036) and Cooperation between Japan and Korea in the Area of Fusion Energy Research and Related Fields. Also, this work is partly supported by the JSPS-NRF-NSFC A3 Foresight Program in the field of Plasma Physics (NSFC: No.11261140328). The authors appreciate the valuable discussions and support of Dr. K. Ochiai at JAEA and FNS team for the experiment at FNS, JAEA.

[1] J. M. Adams *et al.*, Nucl. Instrum. Methods Phys. Res., Sect. A **329**, 277 (1993).
[2] A. L. Roquemore *et al.*, Rev. Sci. Instrum. **61**, 3163 (1990).
[3] M. Ishikawa *et al.*, Rev. Sci. Instrum. **73**, 4237 (2002).
[4] A. V. Krasilnikov *et al.*, Nucl. Fusion **45**, 15039 (2005).
[5] K. Ogawa *et al.*, Rev. Sci. Instrum. **85**, 11E110 (2014).
[6] X. Xie *et al.*, J. Instrum. **11**, C02023 (2016).
[7] J. D. Strachan *et al.*, Phys. Lett. A **66**, 295 (1978).
[8] B. Wolle *et al.*, Nucl. Instrum. Methods Phys. Res., Sect. A **368**, 425 (1996).
[9] M. Isobe *et al.*, Plasma Fusion Res. **8**, 2402068 (2013).
[10] K. Morishima *et al.*, Plasma Fusion Res. **8**, 2402164 (2013).
[11] H. Tomita *et al.*, Rev. Sci. Instrum. **85**, 11E120 (2014).
[12] Y. Nomura *et al.*, Plasma Fusion Res. **6**, 2402148 (2011).
[13] H. Tomita *et al.*, Plasma Fusion Res. **8**, 2406095 (2013).
[14] Y. Nakayama *et al.*, Phys. Procedia **80**, 81 (2015).
[15] Y. Nakayama *et al.*, in *Proceedings on 1st International Conference on Advanced Imaging (ICAI2015)* (The Imaging Society of Japan, Tokyo, 2015), p. 350.
[16] T. Nakamura *et al.*, Nucl. Instrum. Methods Phys. Res., Sect. A **556**, 80 (2006).
[17] K. Morishima and T. Nakano, J. Instrum. **5**, P04011 (2010).